Full paper / Mémoire

Apoferritin as a nanoreactor for preparing metallic nanoparticles

Natividad Gálvez [a,*], Belen Fernandez [a], Elsa Valero [a], Purificación Sánchez [a],
Rafael Cuesta [b], José M. Domínguez-Vera [a,*]

[a] *Departamento de Química Inorgánica, Facultad de Ciencias, Universidad de Granada, Avda Fuentenueva S.N., 18071 Granada, Spain*
[b] *Departamento de Química Inorgánica y Orgánica, E.P.S. de Linares, Universidad de Jaen, 23700 Linares, Spain*

Abstract

Metal (Cu, Co, Ni and Ag) nanoparticles have been prepared within the apoferritin cavity using M^{II}-loaded apoferritin as a chemically and spatially confined environment for their construction. The protein shell prevents bulk aggregation of the metal particles, rendering them water soluble. Optical Ag and Cu nanoparticles showed characteristic surface plasmon resonance whereas magnetic Co and Ni particles confirmed the expected superparamagnetic behavior. *To cite this article: N. Gálvez et al., C. R. Chimie 11 (2008).*
© 2008 Académie des sciences. Published by Elsevier Masson SAS. All rights reserved.

Résumé

On prépare des nanoparticules métalliques (Cu, Co, Ni and Ag) dans la cavité de l' apoferritine. Pour cela on utilise l'assemble l'apoferritine chargée en ion M^{II} comme environnement chimique et spatial. La couche protéique empêche l'agrégation des nanoparticules et les rend solubles dans l'eau. Les propriétés optiques de nanoparticules d'argent et de cuivre montrent la bande de résonance de plasmon de surface caractéristique de ces métaux, tandis que les nanoparticules de cobalt et de nickel présentent le comportement superparamagnétique attendu. *Pour citer cet article : N. Gálvez et al., C. R. Chimie 11 (2008).*
© 2008 Académie des sciences. Published by Elsevier Masson SAS. All rights reserved.

Keywords: Superparamagnetic behavior; Apoferritin; Apoferritin-encapsulated metallic nanoparticles

Mots-clés : Comportement superparamagnetic ; Apoferritine ; Nanoparticules métalliques dedans l'apoferritine

1. Introduction

In the last years, considerable research efforts have been focused on the preparation of water soluble magnetic nanoparticles for their use in biomedical applications as contrast agents in Magnetic Resonance Imaging, drug delivery and hyperthermic treatment of tumors [1,2]. Numerous physical and chemical methods have been employed to produce magnetic nanoparticles [3] focusing on the tight control of particle size and shape. Because of the strong dependence of the magnetic properties on particle size and shape at the nanometer scale, methods yielding uniformly sized and shaped nanoparticles became

* Corresponding authors.
  E-mail address: ngalvez@ugr.es (N. Gálvez).

extremely important. One possible route for obtaining non-aggregated water soluble metallic nanoparticles is the use of a preorganized molecular matrix as a chemical and spatial nanocage for their construction. A typical example of this type of molecule is the iron storage oligomeric protein apoferritin [4] considered as a model for other nanocavity-containing macromolecules such as virus capsides [5]. Apoferritin consists of a spherical protein shell composed of 24 subunits surrounding an aqueous cavity with a diameter of about 8 nm [6]. Channels are generated by the multisubunit construction of the apoferritin shell. Eight hydrophilic channels of about 4 Å allow the passage of metal ions and molecules of sufficiently small size into the cavity of the protein [7].

The first approach to produce apoferritin-encapsulated metallic nanoparticles was the use of the apoferritin cavity for biomimetic oxidative hydrolysis reactions, producing apoferritins reconstituted with non-native inorganic compounds, usually in the form of oxides or oxyhydroxides [8]. A more recent approach is based on the high affinity of some metal ions for the apoferritin cavity [9] and on the capacity of these bonded metal ions to react with an appropriate reagent to produce a metallic particle, constrained to the size of the cavity [11]. Apoferritin has been reported to bind metal ions in its cavity at specific sites, with stoichiometric binding not higher than 60 atoms per apoferritin at pH 7.4 [9]. However, the number of metal ions strongly increases when working at higher pH. For example, when horse spleen apoferritin is treated with Cu(II), Co(II), Ni(II) or Ag(I) and the pH is dynamically adjusted to 8, the number of metal ions per apoferritin reaches values of about 300. Douglas and Ripoll [10] calculated the electrostatic potential in ferritin and found a negative potential gradient directed towards the cavity of the protein supporting the idea of positive ions encapsulation. These encapsulated metal(II)-apoferritins are susceptible of reacting with an appropriate reductant to give rise to the nucleation and growth of a new metal(0)-apoferritin nanoparticle [11]. This last method, therefore, has afforded a wide range of zerovalent metal nanoparticles. The advantage of our procedure lies in the fact that we succeeded in isolating the metal(II) ions-loaded apoferritin species (M^{II}-Apoferritin, see Scheme 1), which, in a second step, can act as nanoprecursor for the preparation of zero-valent metal apoferritin-ecapsulated nanoparticles, avoiding any precipitation outside the apoferritin protein.

Recently, [12] we showed a thorough X-ray near edge structure (XANES) spectroscopy study of the intermediate species (Cu^{II}-Apoferritin) as well as the
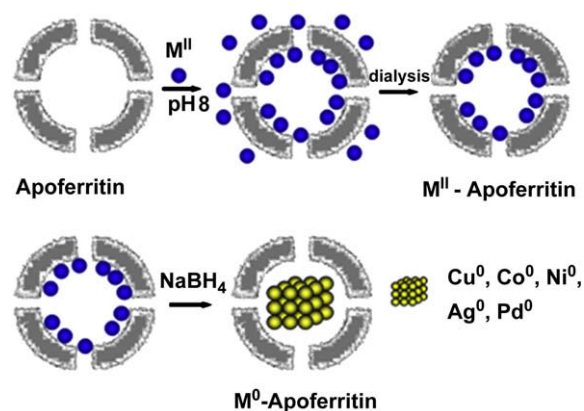
Scheme 1. Schematic representation of the preparation of metallic nanoparticles.

final product Cu^0-Apoferritin which demonstrated that we isolated an Cu-oxide/hydroxide apoferritin species that transformed completely to zero-valent metallic copper apoferritin after reduction with $NaBH_4$.

The aim of this article is to give an overview of the metal nanoparticles preparation method developed in our group.

2. Results and discussion

Apoferritin (Sigma−Aldrich) and M(I) or M(II) were incubated at pH 8 for 24 h. The apoferritin-containing fractions were isolated by G-25 Sephadex chromatography. The M(I) or M(II)-Apoferritin fractions were then monitored by UV−vis spectroscopy at 280 nm and metal determined by atomic absorption spectroscopy (see Section 3). Every collected fraction was added to a $NaBH_4$ solution and then, the apoferritin and metal concentration were measured again, the metal concentration remained the same before and after reduction. The M-associated apoferritin peak (fractions 4−7) is separated from free M^0 (fractions 10−12), which trails well behind (Fig. 1). The coelution of apoferritin and metal (Fig. 1A) indicates that metal clusters are attached to apoferritin. In addition, native apoferritin and M(I) or M(II)-Apoferritin were electrophoretically analyzed on Polyacrylamide gel (PAGE), under native (non-denaturing) conditions (Fig. 1B). The co-migration of the samples (native and M(I) or M(II)-Apoferritins) indicates, first that the protein remained intact after reaction with M(I) or M(II) and second, that M(I) or M(II) atoms are really bounded to the protein.

M(I)- or M(II)-apoferritin acts as a nanoreactor as the trapped M(I) or M(II) ions are able to react with
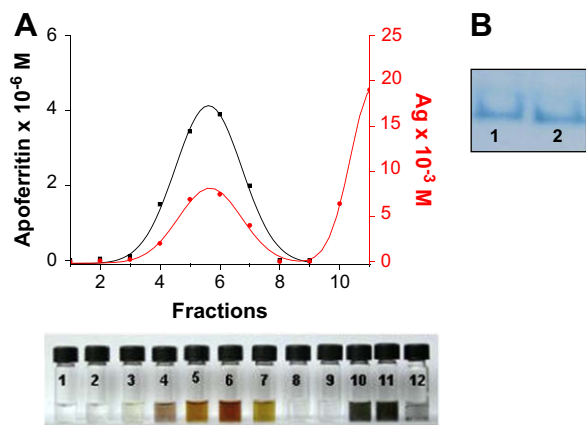
Fig. 1. A. As an example, elution profile of Ag-containing apo-ferritin. Protein was measured by UV−vis spectroscopy and Ag by atomic absorption. B. Native polyacrylamide gel electrophoresis (B) stained with Coomassie Blue. Lane 1 is native apoferritin, lane 2 is M(I)-apoferritin.

a chemical reagent, small enough to traverse the apo-ferritin channels, in this case $NaBH_4$ reductant, to yield a zero-valent metal nanoparticle.

In the case of copper nanoparticles, as a result of the chemical reduction the UV−vis spectrum of the solution dramatically changed, showing the typical absorption band of Cu, centred at 570 nm (Fig. 2A). The observed absorption spectra are similar to those reported for Cu nanoparticles and have been attributed to the plasmon excitation in Cu [13]. Moreover, the band centred at 570 nm appears flattened, which is typical for small clusters [14]. We performed time-dependent formation of Cu in aerobic conditions and its subsequent oxidation was monitored by UV−vis spectroscopy [11]. We observed a decrease in absor-bance at 570 nm and a shift of the SPR position according to the fact that Cu nanoparticles are very

sensitive towards oxidation. The copper oxidation was faster in the absence of apoferritin.

For the Ag nanoparticles the position of the SPR can be tuned by changing particle size, shape, as well as the surrounding dielectric medium. In Fig. 2B, the UV−vis spectrum of the solution corresponding to the particles of 4 nm shows the presence of the SPR at 434 nm. This SPR value is characteristic of Ag particles surrounded with a high refractive index shell [15].

TEM shows the presence of discrete electron-dense spherical cores. The mean diameter was statistically measured to be 3.0 ± 0.5 nm for the case of copper, 4.0 ± 0.5 nm for Ag, 3.5 ± 0.5 nm for Ni and 3 ± 0.5 nm for Co nanoparticles by sampling approx-imately 100 particles. Energy dispersive spectroscopy confirmed the presence of the corresponding metals (Fig. 3). No metals were detected where there were no particles. TEM images of samples negatively stained with uranyl acetate (to visualize the protein shell) confirmed that the particles were actually produced within the apoferritin interior (Fig. 3). The presence of the apoferritin coat prevents irreversible aggregation of the particles and their precipitation.

The magnetic properties of evaporated samples of the Co and Ni nanoparticles were reported [16]. Both of them presented the expected superparamagnetic behavior with blocking temperatures of 70.2 K and 5.9 K, respectively. Clear evidence of the super-paramagnetic behavior of the Co and Ni nanoparticles was given by the ac susceptibility measurements which showed an in-phase (x') and out-of-phase (x'') maxima that shifted towards higher temperatures at increasing frequencies. The superparamagnetic behavior was also confirmed by the field dependence of magnetisation. At temperatures above T_B no hysteresis was observed. In contrast, a clear hysteresis loop of magnetisation was observed below T_B with a coercive field of 39 mT
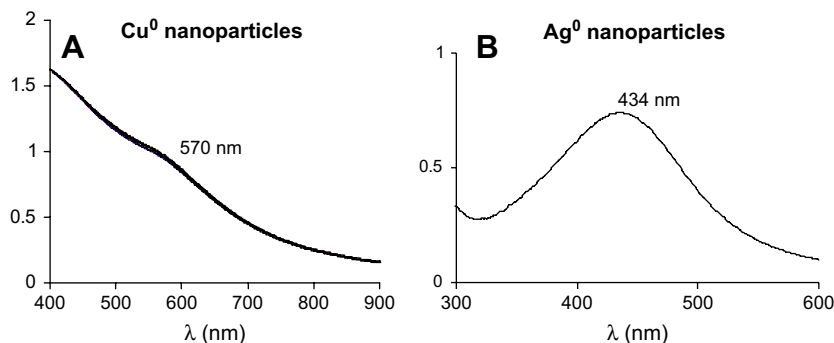

Fig. 2. A. UV−vis spectra of the formation of Cu nanoparticles, showing the flattened band at 570 nm. B. UV−vis spectra of the Ag particles. The SPR shifts to longer wavelength when the size increases from 1 to 4 nm.
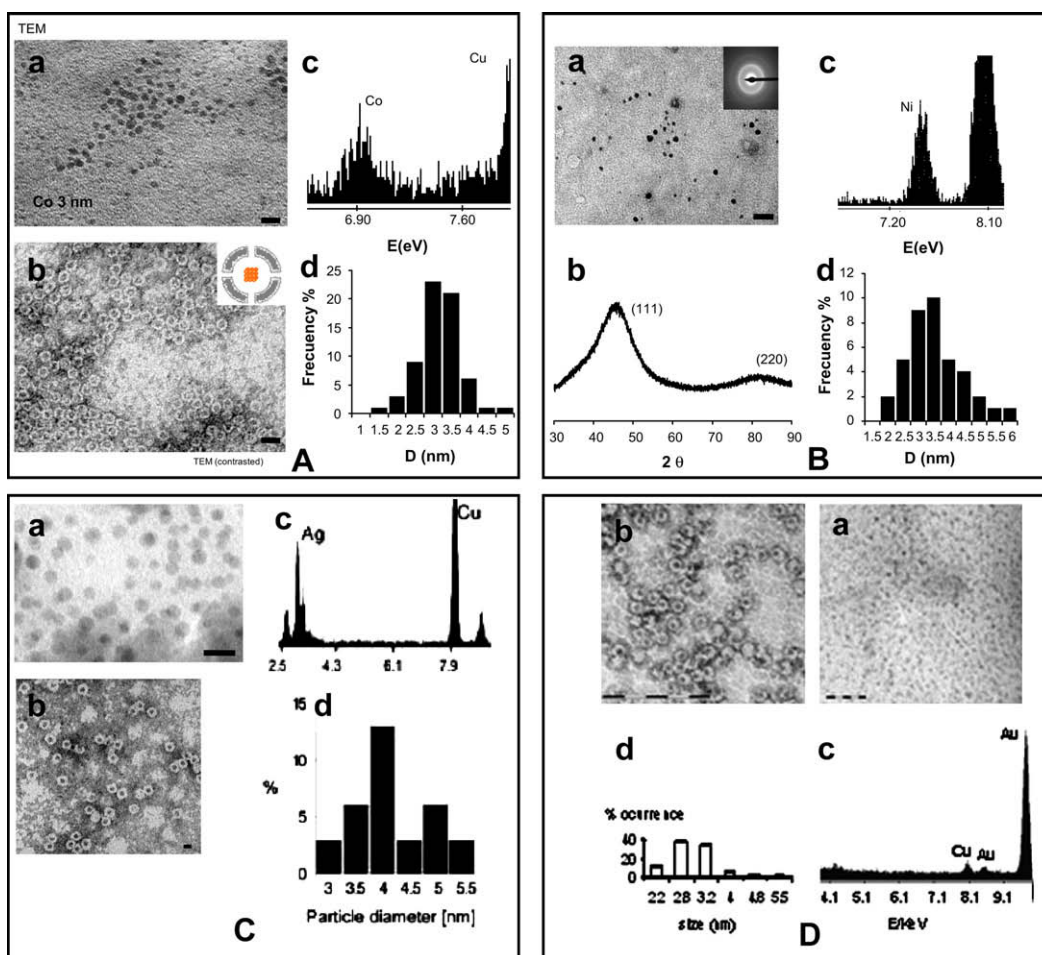
Fig. 3. A. (a) TEM image of Co nanoparticles; (b) negatively stained Co nanoparticles. Scale bars are 10 nm; (c) EDS (Energy Dispersive X-ray Spectroscopy) spectrum; (d) Size-distribution. B. (a) TEM image of Ni nanoparticles. Inset: electronic diffraction pattern of the Ni nanoparticles. Scale bar is 20 nm; (b) X-ray powder diffraction pattern; (c) EDS spectrum; (d) Size-distribution. C. (a) TEM image of Ag nanoparticles; (b) Ag nanoparticles negatively stained with uranyl acetate. Scale bars are 10 nm; (c) EDS spectrum; (d) Size-distribution. D. (a) TEM image of Cu nanoparticles Scale bar is 100 nm; (b) negatively stained Cu nanoparticles. Scale bar is 50 nm; (c) EDS spectrum; (d) Size-distribution.

for Ni and 125 mT for Co nanoparticles at 2 K. We have recently reported that Pd nanoparticles containing ca. 500 atoms (2.4 nm size) encapsulated within the apoferritin cavity show permanent magnetism up to room temperature [16].

Previous works, Watanabe et al. and our group [11,16] showed that different metal ions can be concentrated inside the cavity of the apoferritin molecule and that this apoferritin-loaded molecule can be chemically reduced with $NaBH_4$ to form size constrained metal nanoparticles. In a recent work [12] we performed small angle X-ray scattering (SAXS), X-ray near edge structure (XANES) and extended X-ray absorption fine structure (EXAFS) experiments on the intermediate species (Cu^{II}-apoferritin) as well as the final product obtained after chemical reduction (Cu^0-

apoferritin). The results obtained point out that the encapsulated-Cu^{II} metal ions are in fact a Cu-oxide/hydroxide apoferritin species and that it is completely transformed to a Cu zero-valent metal apoferritin after reduction with $NaBH_4$.

The apoferritin-encapsulated-Cu^{II} oxide and/or hydroxide can act as a reactor because the trapped Cu^{II} ions are able to react with a chemical reagent, small enough to traverse the apoferritin channels, to build a new material. This assumption can be extrapolated to the Ni^{II}- and Co^{II}-apoferritin species.

In conclusion, chemical preparation of Cu, Co, Ni and Ag nanoparticles was carried out using previously M(I) or M(II)-apoferritin as a nanoreactor. Metal and metallic cores of homogeneous size were formed in the apoferritin cavity avoiding agglomeration and bulk

precipitation. The possibility of using the apoferritin cavity as a nanoreactor, opens up the possibility of obtaining a wide variety of metallic nanoparticles of different compositions and homogeneous size.

3. Experimental

Aliquots of 0.1 ml of a 0.1 M MSO_4, ($M = Cu^{II}$, Co^{II}, Ni^{II} and 0.1 M $Ag(NO_3)$ in the case of Ag^{I}) solution were added to a previously chromatographed Sigma–Aldrich Horse spleen apoferritin (4×10^{-5} mmol, 4 ml) to give a theoretical loading of 2000 atoms per apoferritin. The pH was dynamically adjusted to 8 with 0.01 M NaOH. Solutions were then allowed to react at 4 °C for 24 h. The M(I) or M(II)-Apoferritin solutions were then purified by size exclusion chromatography (G-25 Sephadex). The apoferritin-containing fractions were then monitored by UV–vis spectroscopy at 280 nm ($e^{280} = 468,000 \text{ cm}^{-1} \text{ M}^{-1}$) and metal determined by atomic absorption spectroscopy. Addition of $NaBH_4$ (4 mg ml^{-1}) to the solutions of M(I) or M(II)-Apoferritin, produced black solutions of M^0-apoferritin for Cu, Co and Ni, and dark-orange for Ag^0-nanoparticles. Metal determined by atomic absorption spectroscopy after the reduction yielded the same concentration values. The solutions were exhaustively dialyzed against milli-Q water at 4 °C for 12 h. The coelution of apoferritin and metallic ions (Fig. 1A) indicates that metal ions are attached to apoferritin. The purity and stability of the M(I) or M(II)-Apoferritin were assessed by native PAGE. Gels were stained for protein for 1/2 hour using 0.1% Coomassie Blue in fixative 40% MeOH/10% HOAc. Gel was destained by treatment with 40% MeOH/10% HOAc to remove the background during 3 h. The comigration of both (lanes 1 and 2, Fig. 1B) indicates first, that the protein remained intact after M(II) or M(I) loading and second, that the M ions are indeed bounded to the apoferritin.

The samples used for TEM study were prepared by diluting the resulting solutions with milli-Q water and then placing a drop onto a carbon-coated Au or Cu grid and drying it in air at room temperature. The average particle sizes and the standard deviations were estimated from TEM image analysis of 100 particles. Electron micrographs were taken with a Philips CM-20 HR analytical electron microscope operating at 200 keV. X-ray Energy Dispersive Spectroscopy (X-EDS) confirmed that the particles contained the corresponding metals (Fig. 3), which were not detected outside the particles. TEM images of samples negatively stained with 1% uranyl acetate (to visualize the protein shell) confirmed that the particles were actually produced within the apoferritin interior (Fig. 3).

References

[1] R.C. O'Handley, Modern Magnetic Materials, Wiley-VCH, New York, 1999.
[2] (a) P.S. Doyle, J. Bibette, A. Bancaud, J. Viovy, Science 295 (2002) 2237;
(b) H. Gu, P. Ho, K.W.T. Tsang, L. Wang, B. Xu, J. Am. Chem. Soc. 125 (2003) 15702;
(c) D. Wang, J. He, N. Rosenzweig, Z. Rosenzweig, Nano Lett. 4 (2004) 409.
[3] J.M. Perez, F.J. Simeone, Y. Saeki, L. Josephson, R. Weissleder, J. Am. Chem. Soc. 125 (2003) 10192.
[4] (a) E.X. Wu, H. Tang, K.K. Wong, J. Wang, J. Magn. Reson. Imaging 19 (2004) 50;
(b) S.H. Koening, K.E. Kellar, Acad. Radiol. 3 (1996) 273;
(c) D.K. Kim, Y. Zhang, J. Kehr, T. Klasson, B. Bjelke, M. Muhammed, J. Magn. Magn. Mater. 225 (2001) 256.
[5] (a) F. Bertorelle, C. Wilhelm, J. Roger, F. Gazeau, C. Manager, V. Cabuil, Langmuir 22 (2006) 5385;
P.N. Prasad, Mol. Cryst. Liq. Cryst. 446 (2006) 1;
(b) D. Ma, J. Guan, F. Normandin, S. Denommee, G. Enright, T. Veres, B. Simard, Chem. Mater. 18 (2006) 1920.
[6] (a) M. Mikhaylova, D.K. Kim, C.C. Berry, A. Zagorodni, M. Toprak, A.S.G. Curtis, M. Muhammed, Chem. Mater. 16 (2004) 2344;
(b) I. Koh, X. Wang, B. Varughese, L. Isaacs, S.H. Ehrman, D.S. English, J. Phys. Chem. B 110 (2006) 1553;
(c) Y. Sahoo, A. Goodarzi, M.T. Swihart, T.Y. Ohulchansky, N. Kaur, E.P. Furlani, P.N. Prasad, J. Phys. Chem. B 109 (2005) 3879;
(d) S. Santra, P. Zhang, K. Wang, R. Tapec, W. Tan, Anal. Chem. 73 (2001) 4988;
(e) X. Zhao, R. Dytioco, W. Tan, J. Am. Chem. Soc. 125 (2003) 11474;
(f) X. Zhao, L.R. Hillard, S.J. Merchery, Y. Wang, R.P. Bagwe, S. Jin, W. Tan, Proc. Natl. Acad. Sci. U.S.A. 101 (2004) 15027;
(g) S. Santra, K. Wang, R. Tapec, W. Tan, J. Biomed. Opt. 6 (2001) 160;
(h) J. Guo, W. Yang, Y. Deng, C. Wang, S. Fu, Small 1 (2005) 737.
[7] (a) C. Gilles, P. Bonville, K.K.W. Wong, S. Mann, Eur. Phys. J. B 17 (2000) 417;
(b) M. Clemente, E. Coronado, A. Soriano, E. Colacio, J.M. Dominguez-Vera, N. Galvez, R. Madueño, M.T. Martin, Langmuir 22 (2006) 6993;
(c) S.A. Makhlouf, F.T. Parker, A.E. Berkowitz, Phys. Rev. B 55 (1997) R14717.
[8] (a) Y. Li, W. Kim, D. Wang, H. Dai, Appl. Phys. A: Mater. Sci. Process. 74 (2002) 325;
(b) M. Allen, D. Willits, M. Young, T. Douglas, Inorg. Chem. 42 (2003) 6300;

(c) M. Okuda, K. Iwahori, I. Yamashita, Y. Zhang, H. Yoshimura, Biotechnol. Bioeng. 84 (2003) 187;
(d) K.K.W. Wong, S. Mann, Adv. Mater. 8 (1996) 928.

[9] S. Pead, E. Durrant, B. Webb, C. Larsen, D. Heaton, J. Johnson, G.D. Watt, J. Inorg. Biochem. 59 (1995) 15.

[10] T. Douglas, D.R. Ripoll, Protein Sci. 7 (1998) 1083.

[11] N. Galvez, P. Sánchez, J.M. Dominguez-Vera, Dalton Trans. (2005) 2492.

[12] M. Ceolín, N. Gálvez, M.P. Sánchez, M.B. Fernández, J.M. Domínguez Vera, Eur. J. Inorg. Chem. (2008) 795.

[13] C. Salzemann, I. Lisiecki, A. Brioude, J. Urban, M. Pileni, J. Phys. Chem. B 108 (2004) 13242.

[14] U. Kreibig, M. Vollmer, Optical Properties of Metal Clusters, Springer-Verlag, Berlin, 1995.

[15] A.S. Kumbhar, M.K. Kinnan, G. Chumanov, J. Am. Chem. Soc. 127 (2005) 12444;
S. Hussain, R.K. Roy, A.K. Pal, Mater. Chem. Phys. 99 (2006) 375.

[16] T. Ueno, M. Suzuki, T. Goto, T. Matsumoto, K. Nagayama, Y. Watanabe, Angew. Chem. Int. Ed. 43 (2004) 2527;
N. Galvez, P. Sanchez, J.M. Dominguez-Vera, A. Soriano-Portillo, M. Clemente-Leon, E. Coronado, J. Mat. Chem. 16 (2006) 2757;
J.M. Domínguez-Vera, N. Gálvez, P. Sánchez, A.J. Mota, S. Trasobares, J.C. Hernández, J.J. Calvino, Eur. J. Inorg. Chem. (2007) 4823. M. Clemente-Leon, E. Coronado, A. Soriano Portillo, N. Galvez, J.M. Dominguez-Vera, J. Mater. Chem. 17 (2007) 49.